BATTERY TESTERS

SECONDARY CELLS. SEE BATTERY TESTERS. UNINTERRUPTABLE POWER SUPPLIES. SEE BATTERY TESTERS

INTRODUCTION

Electrochemical cells are used to store an amount of electric energy during a charging period and to release this energy at the appropriate time during a discharge period. If a cell is charged by a current I_c then, after a time t, a charge $Q = I_c t$ has been transported through it. Energy is thereby absorbed in the cell since it exhibits a counter-electromotive force (emf.) U_c (Fig. 1a). The operation of electrochemical cells is based on the transformation of material from one chemical form into another and the amount of material transformed is proportional to the charge Q following Faraday's law (1). For completely reversible reactions, the same charge Q will be delivered to the load (dc motor, resistor, etc.) in Fig. 1b after a complete discharge. Since a cell also generates an emf or terminal voltage U_d during discharge, energy is released (1–8). For cells it is common to replace the classic electric charge unit Coulomb (C) by the practical unit ampère-hour (A·h). This unit represents the amount of charge transported when a current of 1 A flows during 1 h and it is the equivalent of 3600 C. The capacity of a cell obtained under nominal conditions of discharge, that is, for a discharge time T_N and a constant current I_N is the nominal capacity $C_N = I_N I_N$. The nominal capacity is, depending on the applications, obtained under specified conditions of temperature, final value U_e of U_d and discharge time T_N. As an example, for lead-acid starter batteries T_N = 10 h with U_e = 1.70 V/cell at 30°C (Deutsche Industrie Normen DIN, Intern. Electrotechnical Committee IEC); for stationary batteries T_N = 10 h, U_e = 1.75 V/cell at 20°C. The nominal current I_N assigned to the nominal capacity follows from $I_N = C_N/T_N$. The rated capacity C_n or n-hour capacity fulfils the equation $C_n = I_n T_n$ wherein T_n differs from T_N. Practice shows that C_N and C_n are different, and this can be attributed to diffusion limitations, pore clogging in the plates of the lead-acid cell at high discharge rates, choice of the final voltage U_e,and parasitic parallel reactions. Other cell chemistries show much less dependence of capacity on discharge current. In general, if I_n is larger than I_N one will see that C_n is smaller than C_N and vice versa. Since electric charge cannot be created or annihilated this means that part of the stored charge could not be accessed ($I_n > I_N$) or was recovered ($I_n < I_N$) from a previous charge-discharge operation. Indeed, the practical Coulombic or A·h-efficiency (charge withdrawn divided by charge necessary to restore this charge) of a charge-discharge cycle can be as high as 95% to 98%, depending on the charging technique used (3, 6). The small loss is due to non-reversible reactions such as hydrolysis of water in the electrolyte or loss of hydrogen in the recombination cycle of nickel-cadmium cells. The capacity of a cell is also a function of temperature and number of charge-discharge cycles. Figure 2 shows generic curves

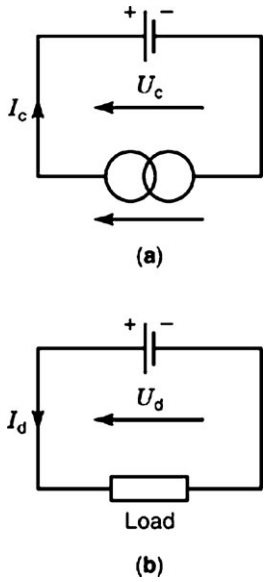

Figure 1. (a) Charging of an electrochemical cell with a current source I_c; the counter-emf. is U_c and power is absorbed. When the cell is discharged (b) in an electric load (resistor, dc motor) with a current I_d the emf. is U_d and power is delivered to the load.Generic curves for the dependence of capacity on temperature for lead-acid and nickel-cadmium batteries. The reference point is the nominal capacity C_N at 20°C.

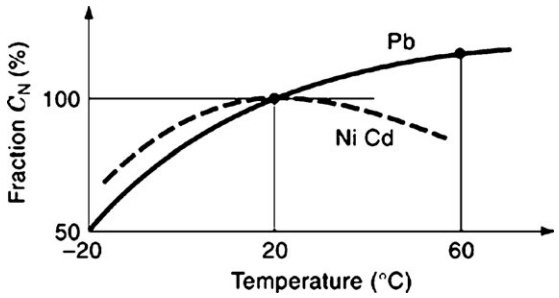

Figure 2. Capacity of lead-acid and nickel-cadmium cells as a function of temperature. The 100% level represents the nominal capacity at 20°C.

for the capacity-temperature dependence of lead-acid and nickel-cadmium cells. The actual shape of the curves is strongly determined by cell construction. The capacity of a cell also varies during its cycle life: Fig. 3 gives the capacity as a function of the number charge-discharge cycles for a given depth of discharge (*DOD*) and fixed operating temperature. During the first cycles capacity increases continuously due to "plate formation", and a value above the 100% level is reached after a few cycles. Further cycling produces a steadily falling curve until cell deterioration becomes so important that the curve finally abruptly falls and the end of life is attained. In practice the 85% level is often chosen as the end-of-life criterion.

Primary electrochemical cells are useless after all their electrode material is consumed by a complete discharge. Some alkaline cells have been redesigned in order to permit a limited number of recharges in combination with a suitable charger, but their cycling performance depends

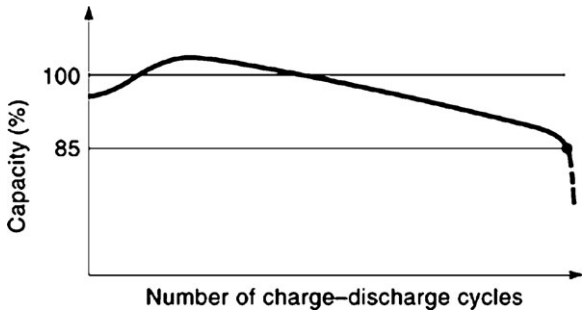

Figure 3. Capacity of a cell as a function of the number of discharge–charge cycles. The capacity initially rises above the nominal capacity level of 100% and then steadily decreases until at the end of the operational life a sudden fall occurs. When the capacity falls below the 85% level the battery is considered to be useless. For vented cells the curve also depends on depth-of-discharge: the deeper discharges shorten cycle life considerably. For VRLA cells the most important failure mechanism is due to corrosion and lifetime is primarily determined by the float conditions.

on the operating conditions during discharge. Secondary cells can withstand a number of charge–discharge cycles because the main electrochemical reactions are reversible. The range of commercially available secondary cells is huge because of the large area of applications. Cells can be combined to form a "battery" in order to increase the output voltage (series connection) or capacity (parallel connection). Small secondary batteries are used on a large scale in portable telephones, laptops, pocket lamps, etc. Since these devices require a long operation time, batteries with very high specific capacity are in favor (lithium-ion, nickel-metal hydride). For starter applications (cars) cheap moderate-power lead-acid batteries govern the market. Nickel-cadmium cells are an alternative for electrical vehicles because of their large specific energy content (2, 6). Heavy stationary lead-acid batteries are used in telephone plants as a buffer between the power and telephone grid. Very-high capacity batteries, applied for power peak shaving in electric grids and that need a very high specific energy content, mostly use a particular chemistry (e.g., sodium-sulfur, redox vanadium).

BATTERY MODELS

The need for a battery measurement is related to the cell or battery models developed by users and researchers. Cell models can be classified as follows (9). Type (a) models, mainly developed for research purposes, permit the understanding of physical, electrical, and chemical phenomena governing the charge–discharge process in a cell or plate. These models use computer simulations and combine diffusion and mass transport equations, electric circuit equations, etc. The equation parameters are determined by matching the measurements with the model, in combination with known experimental data such as the diffusion constant, and acid conductivity law (10–14). Type (b) models are used for the prediction of the stationary charge and discharge behavior of cells or batteries (15) and they mainly rely on the determination of electrical parameters. Typically, the voltage–time discharge curve and the variation law of internal resistance during a discharge of a cell represent examples of such models (16, 17). For lead-acid cells the decrease of capacity with the discharge current is an important phenomenon and this is handled by introducing in the model empirical laws, e.g. Peukert's law (3–18). For the description of the dynamic behavior of a cell or battery, especially for situations in which the discharge current is very irregular as is the case for electric vehicles and photovoltaic systems, the simple type (b) models are insufficient. For this purpose type (c) models are derived from the (b) models by extending the simple electrical models with capacitors and resistors or charge restoration laws (19–23) which permit to include time-dependent effects.

PURPOSE OF BATTERY TESTS

Battery measurements are necessary for the determination of the parameters in a type (a) models or the equivalent electrical parameters in the type (b) and (c) models. The industrial user of batteries, however, desires to replace these extensive and expensive measurements with a simple test in order to specify whether the cell or battery meets a specific criterion. The criterion to be tested depends on the application to be considered. For example, for starter batteries it is important that the internal resistance of the battery is very low in order to obtain a sufficient emf at a high discharge current during a short time, but the rated capacity is irrelevant. In uninterrupted-power-supply applications the battery has to be able to bridge a minimum period under a constant power load, and an almost complete discharge is allowed. Monitoring of a battery consists of a well-defined set of measurements performed over a long period of time with the purpose to determine the long-time behavior of cells and batteries in order to predict premature failures or cycle life. Most battery tests have been developed for lead-acid cells because of their general use in telecommunications plants and the specific problems encountered with this type of cells.

An important reason for performing a battery test is the determination of its state-of-charge (*SOC*) without performing a capacity test. The SOC is the percentage of the actual charge stored in a battery with respect to the assigned n-hour capacity. For example, if a charge of 20 A·h has been drawn from a nominal 100 A·h cell the SOC is 80%. A 100% SOC represents a fully charged battery but does not necessarily mean that it is able to deliver its rated capacity. The 100% SOC condition occurs in the case of batteries permanently fed by a suitable constant voltage U_f and in parallel with a load (Fig. 4). In this float situation one expects the battery to be able to deliver its rated capacity whenever the charger supply voltage is interrupted. Aging or defective cells or wrong float voltages can, however, result in a reduced capacity.

The second reason for testing is to estimate the degree of deterioration or aging or the state-of-health (*SOH*) of the cells of a battery. In lead-acid batteries the aging phenomenon is very complicated and especially batteries subjected to irregular charge-discharge cycles (e.g., in photovoltaic systems, diurnal and seasonal variations of charge

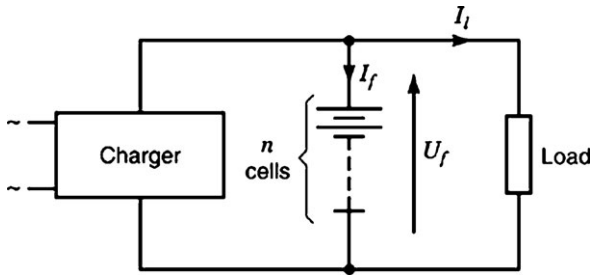

Figure 4. Float charging of a string of n cells in series: battery, load, and charger are in parallel. The charger voltage U_f is chosen so that the battery can be floated permanently without fear for harming it due to the float charge current I_f. The choice of I_f depends on temperature and must assure a 100% state of charge. The average cell voltage is $U_a = U_f/n$. If the supply voltage of the charger is interrupted the battery supplies the load.

and temperature) are often aging in an unpredictable way but their SOH can partly be determined by regular capacity tests. Cells deteriorate because of corrosion of the positive plate grid or shedding of plate material. Shedding is a consequence of the physical changes that occur in a cell plate (volume changes, structural changes, electrolyte transport, gassing) during a charge or discharge. Which mechanism is the worst depends on the type of lead-acid cell and the operating conditions. The classic open cell, in which there exists a connection between the open air and the space above the electrolyte, suffers the most from shedding on the condition that the temperature is below 45°C. Above this temperature the rate of the corrosion reactions becomes very large and the plate grid rapidly deteriorates. Low maintenance cells are classic cells equipped with vent plugs in order to decrease or eliminate water consumption (6, 7). Since 1990 there is a steady increase in the use of sealed valve-regulated lead acid cells (*VRLA*) that are hermetically closed. The internal pressure in a VRLA cell, controlled by a valve, is higher than atmospheric pressure with the purpose to reduce water consumption by enhancement of the recombination reaction of oxygen and protons. During normal operation the valves release minute amounts of gas but when overcharging occurs they act as a safety mechanism and considerable amounts of gas can escape.

It is recommended for VRLA batteries to operate under float charge, and the corresponding float current has to be large enough to ensure 100% SOC for all cells of the battery. As a result of the continuous charge current the internal temperature is a couple of degrees above ambient, and this stimulates plate corrosion.

The third reason for testing a battery is the hope that is is possible to find premature signs of a future occurrence of sudden death failures. This sudden death effect is due to mechanical failures such as bending and shorting of plates, breaks in the connecting road between the plates and the connection posts, growth of crystallines between the two plates (especially nickel-cadmium cells). These faults are, however, the most difficult to predict by testing and manufacturers try to avoid them by a suitable production method and by instructing the user about the best procedure for operating the battery.

BATTERY OR CELL TESTS

Visual inspection

In contrast to maintenance free lead-acid cells and hermetic cells of other chemistries, large open cells of the Planté type are housed in glass containers, and thus it is possible to obtain a visual indication of the state of the individual cells. The color of the plates depends on the SOC and small white points on the negative plate show the existence lead sulfate due to bad floating conditions (2, 3). Differences of the electrolyte levels between cells are suspected. At the bottom of the container, too thick of a layer of sludge indicates that the charge or discharge conditions are too severe. Non-transparent vessels sometimes show a deformed shape because of abnormal plate swelling. The sound from knocking on the cells can be different depending on the quality of the cells. Although this visual inspection seems to be rather crude, when performed by an experienced technician this test can provide more information than simple electrical measurements.

Temperature measurement

Ambient temperature influences the cell temperature and thus the corrosion rate of the plates. Cell temperatures can be measured at the outer side of the container or at the negative connector post for VRLAs. Temperature differences between cells must be within 3°C in order to maintain a full charge with the nominal float current. Especially in badly designed battery rooms or enclosures the temperature of some cells (e.g., in the middle of a cluster) can be much higher than the average, and this results in a reduced life time and an uneven float voltage distribution over the cells. The temperature differences between cells can sometimes be attributed to their specific position in a room. For example, when a number of cells are near a window and in the sun, their temperature will be higher than the temperatures of shaded cells. However, if temperature is higher in some cells without physical reason, an internal cell problem can be the cause.

Specific gravity tests

In lead-acid cells the electrolyte, a mixture of water and sulfuric acid, is an active agent in the cell reactions. The fully charged positive plate consists of lead oxide (PbO_2) with its typical dark brown color, and the discharge causes this material to be transformed into lead sulfate ($PbSO_4$). The fully charged negative plate contains sponge lead (gray) which also transforms into $PbSO_4$ during discharge (1–8). The consequence of this transformation is that the electrolyte becomes diluted since sulfate ions are consumed. The quantity of sulfate ions consumed is proportional to the charge transported through the cell and thus to DOD. The density or specific gravity of the acid is therefore linearly related to the SOC of a lead-acid battery (3, 15). In alkaline batteries the electrolyte only serves as a conducting medium and its density remains practically constant.

The density of the sulfuric acid can be determined with a syringe hydrometer (Fig. 5) or by measuring the electrolyte conductivity. The large amount of acid needed by

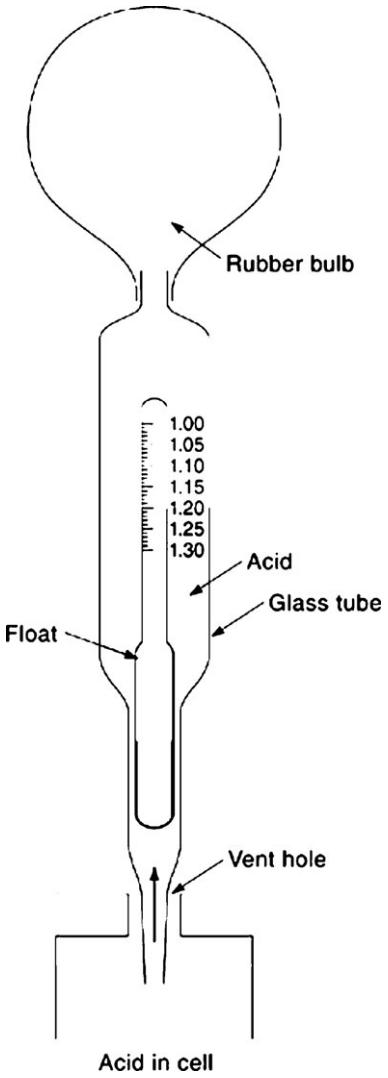

Figure 5. The syringe hydrometer consists of a glass tube, a hydrometer float with engraved scale, and a rubber bulb. The bulb is squeezed and the bottom part of the tube is inserted in the cell electrolyte. Next, the electrolyte is sucked in the tube by releasing the bulb and as a result the level in the tube will correspond with the specific gravity of the electrolyte on the float scale.

the inexpensive syringe hydrometer can be reduced to a few drops if an electronic hydrometer is used. For stationary cells the density (dimensionless) lies in the range 1.200 to 1.225. Starter batteries in cars show values above 1.24 because freezing resistance needs to be higher. Accurate results from a density measurement are only obtained for floating cells. In cycled cells diffusion hinders the immediate mixing of acid in the reservoir between the plates and the diluted acid in the plate pores. Density measurements are also falsified by a tendency of the electrolyte to stratify in the container because of the uneven discharge current distribution over the surface of the plates.

Potentiometric measurements

A potentiometric measurement is mainly used by researchers in order to determine the potential of one electrode with respect to a reference electrode in the electrolyte. In this way the charge-discharge behavior of a single electrode of the cell can be studied without influence of the other electrode. This measurement is impossible in commercial cells because of the small accessible space of acid or their hermetic nature.

Voltage measurements

Open-circuit voltage and float voltage. The open-circuit voltage E_0 of a battery is the terminal voltage when it is disconnected from the load or charger. Since plate potentials are related to the pH of the acid (15) by the equation $E_0 = 2.041\ \text{V} - 0.1182\ \text{pH}$, there exist also a relation with electrolyte density. This relation is for practical purposes given in a linearized form: $E_0 = a + b \times (\text{density})$, wherein the constants a and b are typically $a = 0.93$ V and $b = 0.917$ V. The measurement of E_0 is a substitute for the electrolyte density test, and therefore it is a good indicator for the condition of a stationary lead-acid battery. For instance, too low a value of E_0 after a prolonged charge indicates the possibility of a partial short that increases the self-discharge rate (7). The open-circuit voltage gives, however, only an average indication of acid density since no stratification is taken into account. Diffusion effects in the plates are negligible on condition the battery was at rest for about 24 h before the test. If this is the case, E_0 tends to a rest voltage U_0 that is smaller than E_0.

The average cell float voltage U_a is equal to the charger float voltage U_f divided by the number of cells of the battery. If the individual cell voltages $U_1, U_2, \ldots$ differ too much from U_a a complete system check is necessary (6,7,24). For vented lead-acid cells U_a is about 2.23 V per cell and a deviation of ± 50 mV is acceptable. Larger deviations can be caused by (1) a not completely charged battery after a discharge, (2) defective cells, and (3) a disturbance of the charge-discharge balance due to unnoticed peaks in the consumption that could not be delivered by the charger. For VRLAs the allowable deviations are larger (± 100 mV) and increase at the end of life (7) due to drying out of the plate paste.

Voltage discharge curves. Starting from a fully charged battery a discharge with a constant current is performed and the voltage-time relation recorded. Fig. 6a shows typical curves for different discharge currents I_d for lead-acid and nickel-cadmium cells. At the start of the discharge the voltage drops relatively fast due to the discharge of the double layer capacitor (3, 25) associated with the plates. After these phase the voltage slowly drops during a long time (plateau voltage). For fully charged lead-acid cells a phenomenon called *coup de fouet* can occur at the start of the discharge: the voltage initially dips to a minimum value U_m but recovers to the normal plateau voltage within 10 min [Fig. 6(c)]. This peculiarity is sometimes used as a capacity or SOH prediction test (26, 27). Beyond the knee of the discharge curve, the voltage drops rapidly and the discharge is ended at a given final voltage U_e. It is often advantageous to show the terminal voltage [Fig. 6(b)] as a function of the transported charge $Q = I_d t$. As a matter of fact, if all charge stored in the cells could be retrieved, the

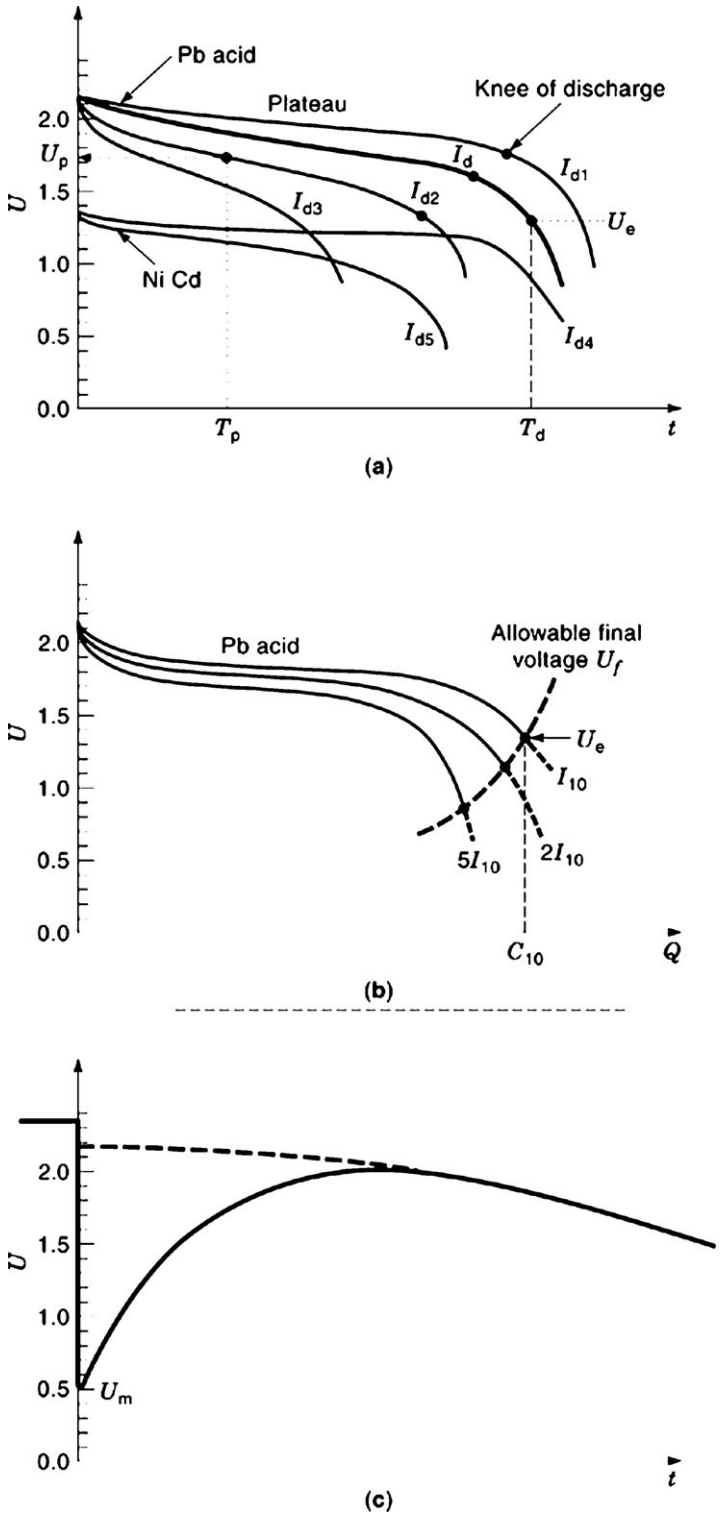

Figure 6. Discharge curves for lead-acid and nickel-cadmium cells with the discharge currents $I_{d1} < I_{d2} < I_{d3}$ and $I_{d4} < I_{d5}$ as a parameter (a). Right from the flat part of the curves (plateau) starts the "knee of discharge" beyond which the terminal voltage falls rapidly. In (b) the x axis is normalized and represents the charge $Q = I_d t$ delivered to the load. The allowable final voltage depends on the discharge current and it determines the dashed line in (b). For a discharge in 10 h (I_{10}) we obtain a capacity C_{10} at the final discharge voltage U_e. In the capacity test the actual operating time T_d is measured at a current I_d; if the terminal voltage U is larger than U_e or T_d is larger than the rated discharge time, the battery passes the test. In (c) the *coup de fouet* phenomenon makes the lead-acid cell voltage drop to a low value U_m at the start of the discharge. After a few minutes the voltage recovers to the normal discharge curve.

curves for different discharge currents should coincide and end at the same capacity (e.g., C_{10}). This not the case for the lead-acid battery due to the previously mentioned effects. For all types of batteries we also have to take into account the effect of internal resistance of the battery on its terminal voltage. This resistance causes a voltage drop proportional to I_d. Otherwise, the internal resistance also tends to increase during discharge, and this imposes a current dependent allowable final voltage. True 100% discharge only occurs when all chemically active material of the plates has been transformed into the discharged state: this does not necessarily correspond with the accepted final voltage. Especially for a lead-acid battery, limitation of U_e to a lower bound is necessary to prevent excessive wear of the cells. Too deep of a discharge induces large volume changes in the plates and favors the formation of a coarse sulfate that

is difficult to reconvert during a charge. This effect is counteracted in VRLAs and rolled-plate-type cells because of the plate compression by the housing. Nickel-cadmium and metal-hydride cells can sustain a deep discharge without harm as long as the polarity of cells in a series chain is not inverted (6).

Battery manufacturers determine voltage discharge curves or discharge tables with the allowable final voltages, and they permit the user to predict the rated capacity at different discharge currents.

Capacity tests. A capacity test of a battery (6) is a discharge test performed under a constant discharge current I_d until after a time T_d (in h) a final terminal voltage U_e is reached. If the resulting capacity $I_d\ T_d$ (in A·h) is larger than the rated capacity, the battery passes the test. The capacity discharge test does not require continuous voltage data collecting; instead it suffices to stop discharge after the trip level for U_e is attained and to measure the corresponding T_d. In particular, one can use specially developed electronic loads for this test. The main disadvantage of this test is that the battery is not able to deliver its rated capacity during and after the test until it is recharged. The capacity test is expensive because it wears down the battery to some extend, it takes several hours, and the stored energy is spoiled. The number of tests must therefore limited to one test every one or two years. Since the probability for a failure increases with time, the frequency of testing may be higher after a few years of operation of the battery. The full capacity test is sometimes replaced by a partial discharge test in order to reduce the loss of system reliability. In practice (28, 29) a 30% to 50% discharge is required for obtaining meaningful diagnostic results. Partial discharge in a floating system can be obtained by decreasing the charger voltage temporarily [e.g., to 46 V for a nominal 48 V system, (30)]. The battery voltage U_p at the end T_p of the test [Fig. 6(a)] gives some information about the state of the battery. If the entire *U-t* curve is recorded during the short time T_p a lot more of information can be obtained. For instance, the presence of the coup de fouet the first minutes indicates that a lead-acid battery is fully charged and well floated and the trough voltage U_m is function of SOC and SOH as already mentioned (25–27).

Current and float current monitoring

Current monitoring is often used to obtain the charge transported through the battery. The discharge current is continuously measured and integrated over time (charge gauging). If the discharge current is fairly constant so that dynamic effects are not relevant, comparison of the rated capacity with the transported charge permits us to estimate the available operating time. If the charge is gauged during the charge period as well it becomes possible to estimate the charging time because of the high A·h-efficiency (95% to 98%). From the estimated SOC of the battery and the rated capacity, the required charge time with a known charge current can be calculated. This avoids heavy overcharging of the battery. However, after a number charge-discharge cycles, due to measurement errors and lack of knowledge of the precise A·h-efficiency (especially near full charge), the deviations between calculated SOC and actual SOC become larger and larger and a reset is necessary, e.g., by giving the battery a full and extended charge.

Float current (I_{fl} in Fig. 4) for floating batteries can also provide diagnostic information (31) but the float current depends on battery temperature and float voltage. Deviations from the normal float current value are suspected if they cannot be related to deviations of ambient temperature or float voltage. The relatively high ratio between discharge or charge current and float current requires different current sensors and increase the cost for these measurements.

Combined voltage and current measurements

Attempts to use battery models for the SOC determination have been made possible by the relative low cost of data collection systems. If the *U-t* discharge curves with parameter I_d are stored as a model of the discharge behavior in a memory, it should be possible to obtain information about SOC from the actual battery voltage and discharge current (17) by comparing these quantities with the stored values. A limited number of curves suffice since intermediate curves can be generated by interpolation (16, 32). Influence of temperature is included by introduction temperature coefficient for the battery voltage. Alternatively, it is possible to use an electrical model of the battery (e.g., Fig. 7) but in practice it can be difficult to assign reasonable parameters to this model because they vary during the course of discharge and charge. Therefore, it is also necessary to tabulate the change of component values with SOC. In both cases the initial discharge data have to be updated after some time, say six months to a year, to take into account aging effects. This of course multiplies the risks of a single capacity test with the number of update discharges. For lead-acid batteries operating with a very varying discharge current, the dynamic effects in the cells are so important that the stored curve method can give rise to large SOC estimation errors. Since the test relies on data of a battery that is in good condition, it can only give significant results when there are no defective cells. It is therefore not suitable as a diagnostic aid.

Impedance and resistance testing

Most of the industrial battery testers rely on the determination of battery internal resistance, conductance, impedance or admittance. The difference between resistance and impedance testing follows from the battery model shown in Fig. 7. In Fig. 7(a), the electrochemical source U_0 represents the ideal energy reservoir, and by neglecting changes in electrolyte density, its value remains constant during the course of a discharge. Resistor R_M represents the resistance of the metallic part of a cell, the sum of (1) the resistances of the connection posts, (2) strap between posts and plates, (3) the plate grid and the interface between grid and the active material. Resistor R_E represents the sum of the resistances of (1) the active electrochemical part of the cell at the interface electrode/electrolyte and separator, (2) the electrolyte, and (3) the plate paste. At very low frequencies a part is due to diffusion effects in the pores of the plates that can only be rep-

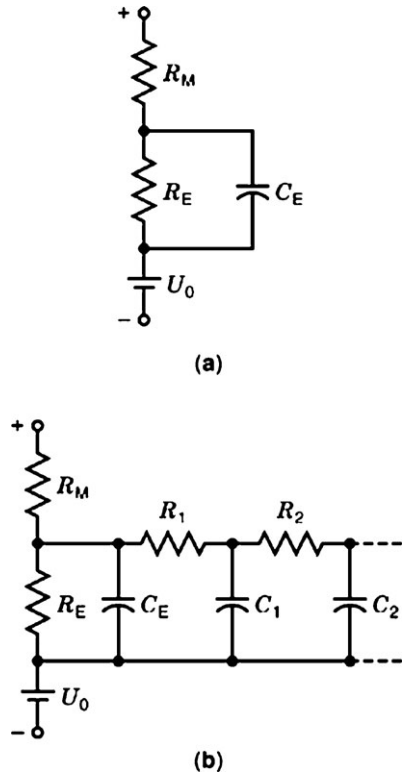

Figure 7. Simple electric equivalent circuits for a cell that can be used for the description of dynamic effects. The resistor R_M represents the sum of the metallic and electrolyte resistances, R_E and C_E are due to the electrochemical double layer on the plates, and U_0 is the rest voltage of the cell. The open-circuit voltage E_0 tends to U_0 after several hours. In (b) R_1, C_1, R_2, C_2 are introduced to obtain a better matching with real impedance behavior.

resented with an infinite chain of capacitors C_1, C_2,... and resistors R_1, R_2,... (19–33). The capacitor C_E represents the double-layer capacitance of the plate interface (about 1.5 F for an 100 A·h cell). The diagnostic value of the impedance tests follows from the fact that some components of this equivalent circuit depend on SOC or change considerably when the cell is aging or deteriorating (34, 35). The resistance R_M increases strongly by corrosion of the posts, the plate grid, and the interface between grid and paste. On the other hand, R_E shows a gradual increase during lifetime for VRLA batteries because there is a continuous loss of water in the paste. Subsequent deep discharge cycles also deteriorate heavily the physical condition of a lead-acid cell, and again this reflects in changes in R_E. In the equivalent circuit of Fig. 7, the parameters are not only determined by construction but also change in time because of the operating conditions. Further, since an impedance measurement gives the sum of the impedances of both plates and the electrolyte between, the component values in Fig. 7 represent an average for the two plates. Without an additional potential electrode in the electrolyte it is impossible to determine the values for the individual plates. One could think that this makes it difficult to extract useful information about the absolute battery condition from impedance measurements. But, in most battery plants the individual cells are operated in a very homogeneous way because of series operation. In the cases when batteries or cells are parallel connected the differences can be much larger. Therefore, it is obvious that deviations of the individual cell parameters from the average obtained from all the cells in a series chain, can produce valuable diagnostic information: cells deviating too much from the average have to be considered as suspect. Practice has shown that this is a good way for separating the good and bad cells of a battery (36–42).

Alternating current impedance tests. The complex impedance **Z** of a battery or cell can be found by forcing a sinusoidal voltage or current into the battery or cells and measuring the amplitude and phase of the corresponding current or voltage. The frequency range of interest for research purposes may be very large: from 10^{-3} Hz to 10^5 Hz. Impedance measurements are popular because testing is fast, there is no discharge of the battery during the test, and it can remain in operation. Standardization of the measurement conditions is necessary, and therefore a rest period of 2 h to 4 h before the test is recommended. The temperature should be stabilized and preferably about 21°C. Figure 8 shows typical curves of the real part and phase-angle of **Z** as a function of frequency. It is seen that, in accordance with the equivalent circuit, a cell behaves capacitively below 10 Hz and resistively somewhere between typically 10 Hz and 100 Hz (6, 43). Above this frequency the inductive component of ***Z*** due to the inductance of the posts, straps, and plates becomes predominant. This higher-frequency region is not important for testing since it gives little or no information about the condition of the plates. The minimum value of $|\mathbf{Z}|$ is always found in the resistive region. The "ohmic resistance" (R_i) is the value of $|\mathbf{Z}|$ at a phase-angle zero, determined from the phase-angle curve. In general it is seen that this frequency decreases somewhat with increasing nominal capacity. A single ideal measurement frequency for all batteries can therefore not be found. Figure 9 shows the behavior of impedance as a function of SOC and with the measurement frequency as a parameter (43). From 0% to 80% SOC we see that $\log|\mathbf{Z}|$ falls almost linearly with SOC. Above 80% an increase occurs due to gassing or gas recombination. A correlation exists between $|\mathbf{Z}|$ and SOC for all lead acid cells but the dispersion on the measurements between different cells is larger than the variations in $|\mathbf{Z}|$ due to SOC in the range above 80%, and actually this is the most important region for floating batteries. The effect of temperature on the $|\mathbf{Z}|$ measurements can be neglected. VRLAs show a marked increase of the real part of **Z** at the end of their life. If the real part and absolute value of the imaginary part of **Z** are drawn in the complex plane and with frequency as a parameter (Cole-Cole plot, Fig. 10), the typical half-circle shape at medium frequencies and the straight line for low frequencies is the result (21–44).This is due to kinetic effects at the electrical double layer of the plates Analysis in this region is difficult because no universal equivalent circuit exists at the moment (6). A very low test frequency would also result in unduly long measurement times. The determination of conductance from the real part of the admittance $\mathbf{Y} = \mathbf{1/Z}$ or by direct measurement leads to similar results.

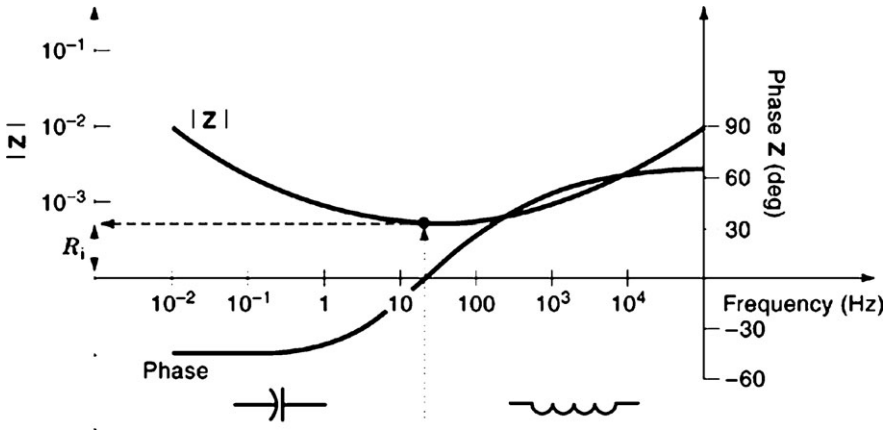

Figure 8. Generic curve for $|\mathbf{Z}|$ and the phase of the cell impedance as a function of frequency. The $|\mathbf{Z}|$ scale is logarithmic but the units are arbitrary; the frequency scale is logarithmic. In the range 10 Hz to 100 Hz the cell behaves resistively and the corresponding value is the ohmic resistance (R_i). Below this frequency the cell reacts capacitively and above inductively.

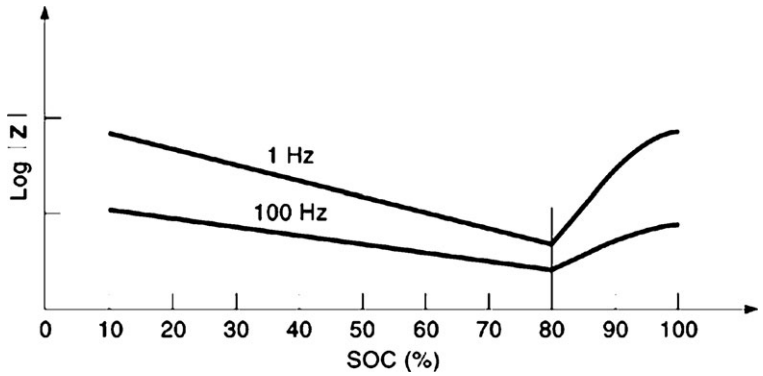

Figure 9. Generic curves for $|\mathbf{Z}|$ (logarithmic scale) as a function of state of charge and with frequency as a parameter. From SOC = 80% on $|\mathbf{Z}|$ increases because of gas generation on the plate surfaces.

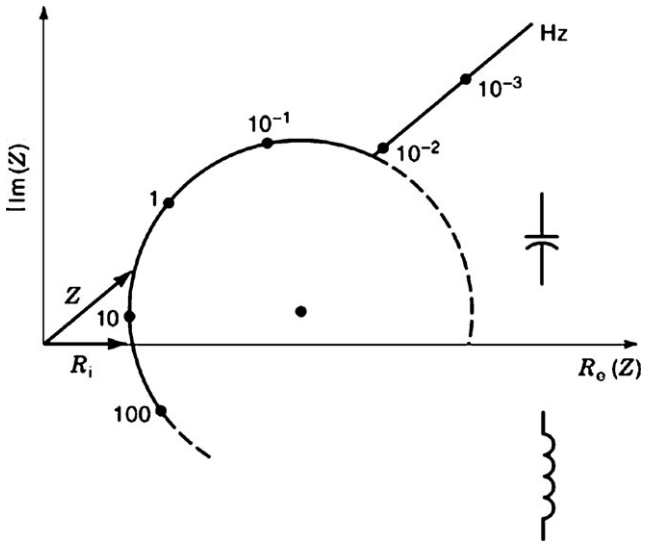

Figure 10. Cole-Cole plot for the impedance **Z**: real part of **Z** and absolute value of the imaginary part with frequency as a parameter. The straight line at very low frequencies is due to diffusion effects at the double layer capacitor of the plates; the circular part is result of C_E and R_E. The ohmic resistance R_i is found on the real axis. Above the real axis the cell behaves capacitively and below inductively.

There exist several possible practical impedance test implementations for on- and off-line batteries.

1. Injection of an ac sinusoidal current (45, 46) with amplitude I in a cell. If the resulting ac voltage amplitude E [Fig. 11(a)] is measured, then $|\boldsymbol{Z}| = E/I$. In general, it is difficult or impossible to inject a current in the battery when it is floating due to the low charger impedance. However, if it is injected in a single cell, the other cells will separate it from a constant voltage charger by virtue of their internal impedances. For a series chain of 24 equal cells (nominal 48 V battery) only 4.2% of the injected current will be diverted to the other cells in the chain if all internal resistances are about equal. More complex systems use a synchronous detector for the determination of E so that the complex value **Z** is obtained. The measurement frequency (typically 37 Hz to 73 Hz) must not be harmonically related to the mains frequency (50 Hz or 60 Hz) so that the synchronous detector can completely eliminate the charger ripple.
2. If the charger ripple current is not too large the resulting voltage ripple over the battery or cells is proportional to the internal impedance. The ripple current can be measured with an ac current probe or

shunt (47) and the voltage with a sensitive ac voltmeter [Fig. 11(b)]. One has to interpret the results of this measurement very carefully. First, the voltage-current curve of a cell (3, 48) is not linear (Fig. 12) and the voltage waveform therefore differs from the current waveform if the amplitude of the latter is very large. But, for not too large a ripple current the ripple voltage is approximately proportional to the current. Second, if the ripple current is not sinusoidal, a Fourier series can represent it. Since **Z** is complex and depends on test frequency, the Fourier components of the ripple voltage series will differ from those in the current series. Therefore it is recommendable to selectively measure the amplitudes of the fundamental waves of current and voltage ripple and calculate |**Z**| from their ratio. Alternatively, if a data collection system is available, a fast Fourier transform (*FFT*) can be performed on the data of current and voltage. In this method one is, however, limited to discrete frequencies, that is, the multiples of the ripple frequency (49). If the battery is discharging and the discharge current shows a stochastic pattern then sampling the current and voltage at regular intervals can also lead to an impedance value if again a FFT is performed on the samples. In this case a more uniform spectrum can be obtained. The latter methods require, however, expensive and complex measurement equipment.

3. The three-voltmeter method is a classic method (50) and is implemented as follows (51): an ac current with a value of 8 A to 9 A is injected in a cell and the effective value I_e of this current is measured with an ac current probe instrument. The connection wire (b_k,a_{k+1}) between two cells with position number k and k+1 is now used as a reference resistor (Fig. 13). Next, three *effective* voltages are measured: U_1 between a_{k+1} and b_k, U_2 between a_k and b_k of the cell k,and the total voltage U_3 between a_k and a_{k+1}. The real part R of the cell impedance $\boldsymbol{Z}$ then follows from:

$$R = \frac{U_3^2 - U_2^2 - U_1^2}{2U_1 I_e}$$

Although the voltages are small (1 mV to 2 mV) a modern instrument with true root-mean-square (rms) capability suffices. In principle, it is also possible to calculate the phase of **Z** from the three voltages, but this supposes a pure sine-wave excitation and a linear voltage-current curve. The reproducibility of this method is excellent and the test can be performed with the battery on- or off-line. The measuring equipment is standard and it is possible to use the rectifier ripple current on the condition it is large enough.

Pulse-impedance and dc load tests. Pulse-impedance and dc-load tests permit us to determine in a fast way the internal resistance or conductance of a cell.

Load voltage test. This is one of the oldest methods for the determination of internal resistance. A cell of the battery is first loaded with a current I_1 and a terminal voltage

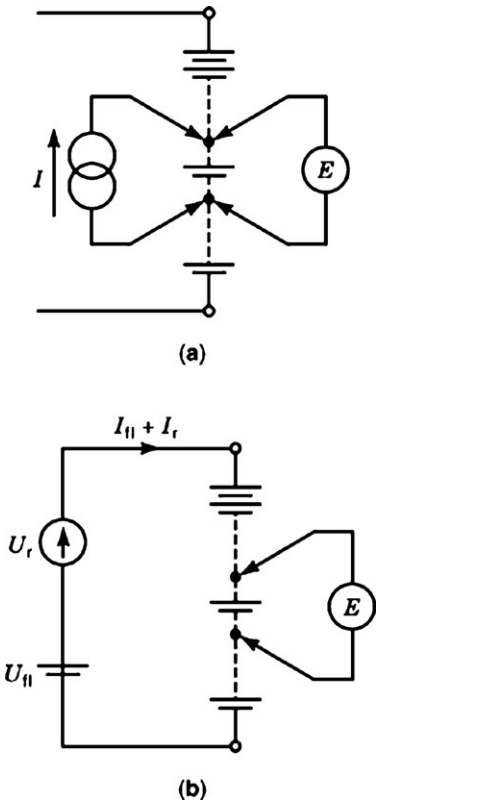

Figure 11. Measurement of the internal impedance of a cell: an ac current I is forced into the cell and the resulting ac voltage E is measured. In (b) the ripple voltage U_r superposed on the charger float voltage is used as a source. The resulting battery current ripple value I_r is measured with an ac current probe or current shunt and the ac ripple voltage over a cell with an ac voltmeter E. The source U_{fl} represents the dc part of the float voltage.

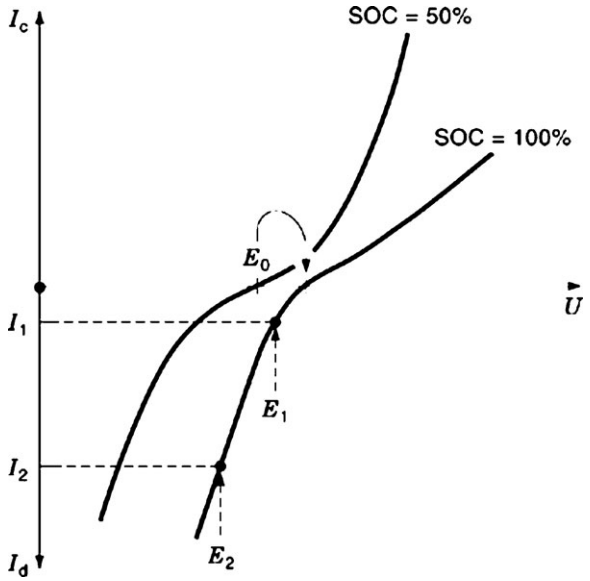

Figure 12. Nonlinear current–voltage curve of a cell for charge (I_c) and discharge (I_d) currents and for 50% and 100% state of charge. The equilibrium voltage at $I_c = I_d = 0$ shifts to the right when SOC increases because acid density increases.

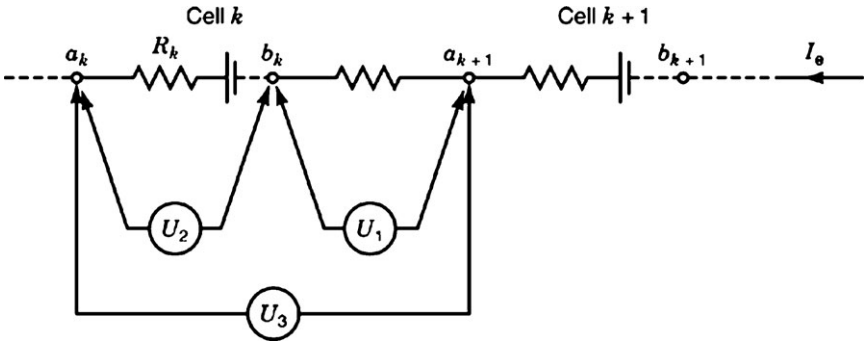

Figure 13. Three ac rms. voltage measurements U_1, U_2 and U_3 and knowledge of the rms. ripple current value I_e permit to determine the real part of the cell impedance in a string (here shown for cell k).

U_1 is measured. Next, the load current is increased to I_2 and reading U_2 results. From these values a resistance R_i is defined:

$$R_i = -\frac{U_2 - U_1}{I_2 - I_1} = -\frac{\Delta U}{\Delta I}$$

Because of the nonlinear voltage-current characteristic of the battery it is necessary to standardize the load currents in order to obtain comparable results. Suitable values are $I_1 = 0.2$C and $I_2 = 4.2$C with C the capacity of the battery in A·h and I_1 and I_2 in A. The definition of R_i corresponds with the inverse slope of a straight line connecting the two measurement points in the voltage-current characteristic of Fig. 12. The voltage-current curves are different for a discharge and charge current, especially at the end of the charge mainly because of the gas generation on the plates. Therefore it is recommendable to perform the load voltage test under discharge. The R_i value obtained gives a good measure for the resistance of the metallic part of the battery or cell if the measurement time is much shorter than the time constant due to R_E andC_E (5 min to 10 min) of Fig. 7(a). Because R_i depends on SOC it is common to start with I_1 from a fully charged battery. A disadvantage of this method is the large discharge current I_2, for example, 420 A for a 100 Ah battery. An expensive load resistor or active load with additional cabling is thus required. The capacity loss of the cell during the measurement remains small because the load time is short.

Current pulse test. In this test (51) a current pulse ΔI is superposed on the normal charge (or discharge current) for a fixed time (3 s to 10 s). The battery reacts to this pulse by increasing (or decreasing) its terminal voltage (Fig. 14). In Ref. (52) it is proposed to use a charge current I_5 and a pulse $I = 2\ I_5$. The voltage U_1 at the end of the pulse and U_2 immediately after the pulse is measured. The battery is then left to rest for 30 minutes and a third reading U_3 is obtained. From this voltages one can define three resistance values: $R_1 = (U_1 - U_2)/I$, $R_2 = (U_2 - U_3)/I$ and $R_3 = (U_1 - U_3)/I$. The equivalent circuit of Fig. 7(a) shows that the voltages U_1 at the end of the current pulse and U_2 immediately after the pulse are different due to voltage drop over R_M ($= R_1$). The value R_2 has relation with the electrochemical phenomena at the double-layer surface; the slowly dropping voltage during the rest period is due to C_E and R_E. After about 30 minutes the transient current through C_E has vanished and we find $R_E = (U_2 - U_3)/I$. Resistance R_3 is a combination of both effects. Experiments have shown that the results obtained have a similar shape as a function of DOD and that there is a strong correlation with a pure ac impedance method. In (53) the battery is subjected to a 72 A discharge pulse I for 3 s to 10 s and U_1, U_2 or U_3,U_4 are measured (Fig. 15). It follows that $R_M = (U_1 - U_2)/I = (U_4 - U_3)/I$.

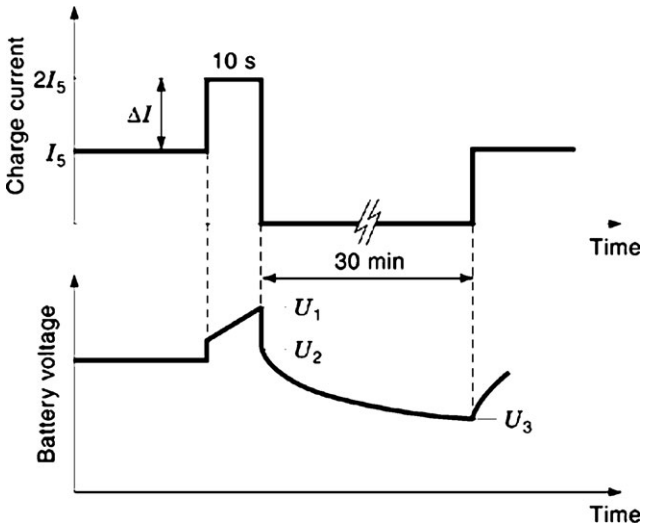

Figure 14. Determination of internal resistance by a 10 s pulse current superposed on the charge current (I_5). The battery is then left at rest for 30 min and from U_1, U_2 and U_3 follow R_M and also R_E.

Current impulse test. In the current impulse test (45) the cell is loaded during a very short period (500 μs) with a current impulse (e.g., $I_{6.6}$) and the voltage U_1 just before the start of the impulse and U_2 at the end of the impulse are measured. The metallic resistance is $R_M = (U_1 - U_2)/I_{6.6}$ and it appears that this value permits to estimate the SOC within a 10% error. The advantage of this method is a very low discharge dissipation and capacity loss.

Other tests.

1. Noise voltage tests. It is well known that complex electrochemical reactions produce electrical noise (54). There have been several attempts to apply this property for diagnostic purposes in batteries (55) or

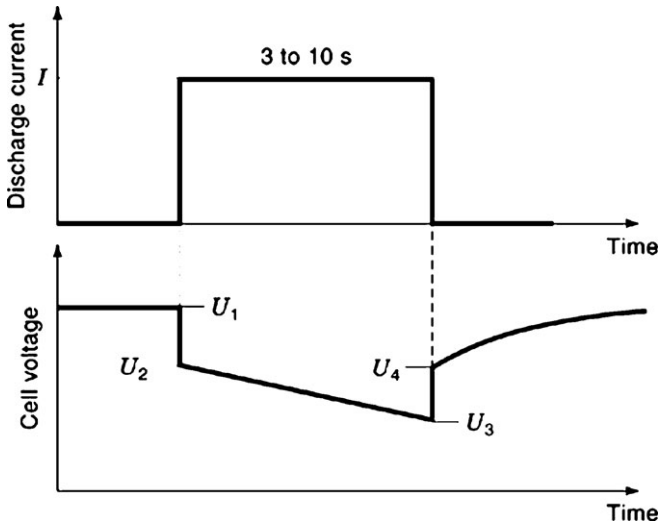

Figure 15. Variant of Fig. 14: a pulse discharge current is applied during 3 s to 10 s and U_1, U_2 or U_3, U_4 are measured. From the differences $U_1 - U_2$ or $U_4 - U_3$ follows R_E.

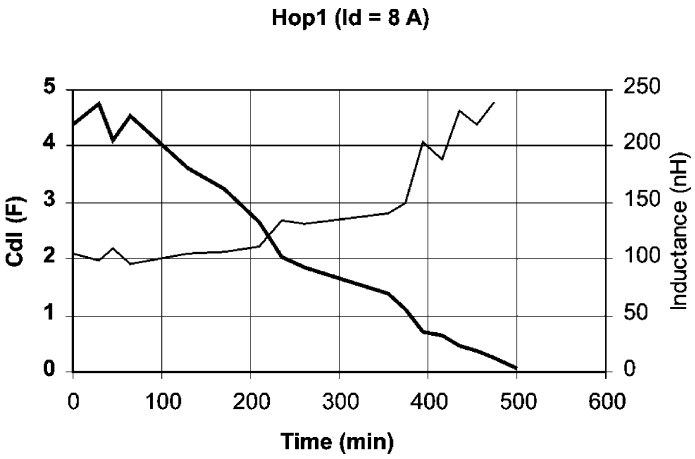

Figure 16. Double-layer capacity C_{dl} and internal inductance during the course of a constant current discharge at 8 A for a 6 V/100 A·h VRLA battery. The same shape of the curves is seen for nickel-cadmium cells.

SOC determination (56). Measurements (57) show that the open circuit noise voltage of a cell increases when the SOC decreases, probably because the internal resistance is responsible for a part of the noise voltage. There is also a correlation between the open circuit voltage noise level of a fully charged cell at rest and the state-of-health. When current flows in the cell the noise voltage increases because of the electrochemical reactions. The noise level effect is especially large for primary cells because of the large internal resistance. The noise voltage measurements are applicable to different cell chemistries since the noise is an intrinsic property of an electrochemical reaction. A disadvantage is that noise measurements are not easy to perform: a complex instrument setup is required and the results are sensitive to electromagnetic interference produced in the environment of the cells.

2. Measurement of the electric capacitance. The component values of the equivalent circuit in Figure 7 depend on the SOC of a cell. Since the cell reactions occur at the active surface of the electrodes, the values of C_E, C_1, etc. will be proportional to this active surface and thus to the SOC. Detailed analysis of the plate reactions requires the knowledge of the entire Cole-Cole plot of Figure 10. This plot can be determined by electrochemical impedance spectroscopy (*EIS*). Because EIS requires a very long measurement time and expensive equipment and gives in fact more information than is wanted for technical applications, simplification is possible. The capacitors C_1, C_2, etc. in Figure 7(b) are indeed related to the slow diffusion effects in the active mass of the plates while C_E is a function of the double layer capacitance of the active electrode surface. In (58) it is reported that the continuous EIS frequency spectrum can be replaced by measurements at twenty four frequencies from 20 Hz to 2000 Hz for the determination of cold cranking amperes of starter batteries. A further reduction to three frequencies has been proposed in (59) and the results reveal the linearity between SOC and C_E. Finally a measurement at a single frequency still gives acceptable results (60). If this measurement is performed at the internal resonance frequency of the cell it is also possible to determine the internal inductance of a cell. Figure 16 shows a result we obtained with this method. The variation of the internal inductance with the SOC is similar to the variation of the internal resistance but the sensitivity to SOC is larger. All this capacitance methods are applicable to lead-acid and NiCd cells. For the primary Zn-MnO_2 elements the linearity between SOC and C_E is disturbed by the heavy change of the Zn-electrode roughness.

INTERPRETATION OF THE MEASUREMENTS AND TESTS

For small and cheap batteries the full capacity test suffices to obtain an indication of the state of the battery. In contrast, for the large industrial installations it is difficult to perform this test and we have to rely on a thorough monitoring of float current of the battery and cell voltages. The following principles can be used for diagnosing of cell failures. A single deviation of a parameter of a cell from the average value does not necessarily mean that the cell is deficient. If this deviation can be related to deviations of other operating parameters (temperature, unexpected discharges, etc.) the cell is probably good but needs conditioning. If this is not the case, there exists a change in the operating conditions of the cell, for example, because of fast aging. It is important to store the baseline values of parameters such as temperature, cell voltage, and float current at the start of operation of a new battery. The actual electrical parameter values depend on the state of the cells: charged, discharged, floating, lifetime, cycle life, etc. It is better to compare ratios of related parameters than to

rely on the actual values. If, for example, the load current increases with ΔI, then the terminal voltage will increase with ΔU and one expects the ratio $\Delta U / \Delta I$ to remain almost constant. If the float charger voltage increases, then the minimum (or maximum) of the individual cell voltages will also increase, but the ratio float voltage to minimum (maximum) will almost be constant. A thermally unstable cell will show a higher ratio of cell temperature to ambient temperature. The diagnostic value of these tests is much enhanced when they are combined with impedance or resistance measurements.

CONCLUSIONS

The most important parameter of a battery is its rated capacity, which can only be determined under real conditions. Alternative tests have the purpose to estimate the condition of a battery or individual cells but it remains almost impossible to predict sudden death of cells.

In (53) the following conclusions are drawn: (1) no test can replace the capacity test, (2) a capacity test is expensive but a battery is costly and therefore the test is worthwhile, (3) for small systems with not too high a degree of required reliability, it is allowed to replace the capacity test with the impedance test, (4) when in large systems some cells show too large an impedance deviation from the mean value, there is a chance that a serious failure exists and a capacity test is necessary, and (5) conductance tests have to be performed with the battery fully charged.

BIBLIOGRAPHY

1. J.C. Kotz, K.F. Purcell, *Chemistry and chemical reactivity*, 2nd ed., Philadelphia: Saunders College, 1991.
2. G.W. Vinal, *Storage Batteries*, 4th ed., New York: Wiley, 1954.
3. H. Bode, *Lead-Acid Batteries*, New York: Wiley, 1977.
4. M.A. Dasoyan, I.A. Aguf, *Current Theory of Lead Acid Batteries*, Stonehouse, UK: Technicopy, 1979.
5. M. Barak, *Electrochemical Power Sources*, London: The Institution of Electrical Engineers, 1980.
6. D. Berndt, *Maintenance-free Batteries*, Somerset, England: Research Studies, 1993.
7. W. Fischer, *Stationary Lead-Acid Batteries: an Introductory Handbook*, Brilon, Germany: Hoppecke, 1996.
8. C.A. Vincent, B. Scrosati, *Modern Batteries*, New York: Wiley, 1997.
9. D. Baert, A. Vervaet, Lead-acid battery model for the derivation of Peukert's law, *Electrochem. Acta*, **44**, 3491–3504, 1999.
10. J. Bouet, J.P. Pompon, Analyse des causes de dégradation des plaques positives de batterie au plomb, *Electrochem. Acta*, **26**(10): 1477–1487, 1981.
11. P. Ekdunge, D. Simonsson, The discharge behaviour of the porous lead electrode in the lead-acid battery, *J. Applied Chem*., **19**, Part I: 127–135, 1989, **19**, Part II: 136–141, 1989.
12. H. Lehning, Beitrag zur mathematischen Beschreibung der elektrochemischen Vorgänge im Bleiakkumulator, *Elektrotech. Z. A*, **93**, 62–66, 1972.
13. Gu Hiram, T.V. Nguyen, R.E. White, A mathematical model of a lead-acid cell, *J. Electrochem. Soc.*, **134**(12), 2953–2960, 1978.
14. P. Ekdunge: A simplified model of the lead/acid battery, *J. Power Sources*, **46**, 251–262, 1993.
15. W.A. Facinelli,Modeling and simulation of lead-acid batteries for photovoltaic systems, Ph. D. dissertation, Arizona State University, 1983.
16. C.M. Sheperd, Design of primary and secondary cells, II, An equation describing battery discharge, *J. Electrochem. Soc.*, 657–664, **112**, 1967.
17. E. Ofry, S. Singer, Measurement of the state of battery charge using an improved loaded voltmeter test method, *IEEE Trans. Instrum. and Meas.*, **IM-31**(3), 154–158, 1982.
18. D. Mayer, S. Biscaglia, Use of modeling of lead-acid battery operation for the development of a state charge meter, *Proc. IEEE Tenth European Photovolt. Solar Energy Conference*,April, Lisbon, Portugal, 1209–1213, 1991.
19. J. Appelbaum, R. Weiss, Estimation of battery charge in photovoltaic systems, *Proc. IEEE Sixteenth Photovolt. Specialists Conf.*, 304–307, 1982.
20. J. Appelbaum, R. Weiss, An electrical model of the lead-acid battery, *Proc. Int. Telecommun. Energy Conf. (INTELEC)*, Washington D.C., Oct., 304–307, 1982.
21. P. Mauracher, E. Karden, Dynamic modeling of lead-acid batteries, *J. Power Sources*, **67**, 69–84, 1997.
22. J. Heldt, W-R Canders, Eine experimentell gestützte Simulation der Bleibatterie als Energiespeicher für Elektrofahrzeuge, *Elektrotechn. Z. A*, **99**, 342–347, 1978.
23. W. Runge, Die Berechnung des Stationären und Dynamischen Entladeverhaltens von Bleiakkumulatoren, *Archiv Elektrotech.*, **57**: 235–246, 1975.
24. D. Berndt, *Maintenance and reliability of stationary batteries*,Varta Spezial Report, 1, 1985.
25. Z. Nworolski, U. Reskow, Dynamic properties of lead acid batteries:Part I, initial voltage drop, *Proc. Int. Telecomm. Energy Conf.*, Vancouver, Canada, Oct., 1998, 215–220.
26. Ph.E. Pascoe, A. Anbuky, Estimation of VRLA battery capacity using the analysis of the coup de fouet region, *Proc. Int. Telecomm. Energy Conf.*, Copenhagen, Denmark, June 1999, Session 6-1.
27. C.S.C. Bose, F.C. Laman, Battery state of health estimation through coup de fouet, *Proc. Int. Telecomm. Energy Conf.*, Phoenix, AZ, Sept. 2000, 597–601.
28. Kurisawa, M. Iwata, Capacity estimating method of lead-acid battery by short-time discharge, *Proc. Int. Telecomm. Energy Conf.*, Melbourne, Australia, Oct. 1997, 483–490.
29. Suntio, Imperfectness as a useful approach in battery monitoring, *Proc. Int. Telecomm. Energy Conf.*, Vancouver, Canada, Oct. 1994, 481–485.
30. G.A. Pederson, The use of ratiometric measurements to determine battery status, *Proc. Int. Telecomm. Energy Conf.*, Vancouver, Canada, Oct. 1994, 491–496.
31. K.D. Floyd, Z. Noworolski, J.M. Noworolski, W. Sokolski, Assessment of lead-acid battery state of charge by monitoring float charge current, *Proc. Int. Telecomm. Energy Conf.*, Vancouver, Canada, Oct. 1994, 602–608.
32. D. Baert, End-of-charge and discharge criterion for batteries, *Proc. Int. Telecomm. Energy Conf.*, Paris, Sep. 1993, 431–434.
33. P. Bro, S.C. Levy, *Quality and Reliability Methods for Primary Batteries*, New York: Wiley, 1990.

34. F.J. Vaccaro, P. Casson, Internal resistance: harbinger of capacity loss in starved electrolyte sealed lead acid batteries, *Proc. Int. Telecomm. Energy Conf.*, Stockholm, Sweden, June 1987, 128–131.
35. S.L. DeBardelaben, A look at the impedance of a cell, *Proc. Int. Telecomm. Energy Conf.*, San Diego, Oct. 1988, 394–397.
36. M. Kniveton, A.I. Harrison, Impedance/conductance measurements as an aid to determining replacement strategies, *Proc. Int. Telecomm. Energy Conf.*, San Francisco, Oct. 1998, 297–301.
37. M. Hugues, R.T. Barton, S.A.G.R. Karunathilaka, N.A. Hampton, The residual capacity estimation of fully sealed 25 Ah lead/acid cells, *J. Power Sources*, **17**, 305–329, 1986.
38. B. Jones, Conductance monitoring of recombination lead acid batteries, *11th International Lead Conference*, Venice, Italy, May 1993.
39. D.O. Federer, Th.G. Croda, K. Champlin, M.J. Havlic, Field and laboratory studies to assess the state-of-health of valve-regulated batteries: Part I, Conductance/capacity correlation studies, *Proc. Int. Telecomm. Energy Conf.*, Washington D.C., Oct. 1992, 218–233.
40. M.J. Havlac, D.O. Feder, Th.G. Croda, K. Champlin, Field and laboratory studies to assess the state-of-health of valve-regulated lead acid and other batteries technologies: Part II, Further conductance/capacity correlation studies, *Proc. Int. Telecomm. Energy Conf.*, Paris, Sept. 1993, 375–383.
41. M.J. Havlac, D.O. Feder, Analysis and interpretation of conductance measurements used to assess the state-of-health of valve regulated lead acid batteries, *Proc. Int. Telecomm. Energy Conf.*, Vancouver, Canada, Oct. 1994, 282–291.
42. W.H. Edwards, A.I. Harrison, T.M. Wolstemholme, Conductance measurements in relation to battery state of charge, *Proc. Int. Telecomm. Energy Conf.*, Copenhagen, Denmark, June, 1999, item 18.3.
43. J.M. Hawkins, L.O. Barling, Some aspects of battery impedance characteristics, *Proc. Int. Telecomm. Energy Conf.*,The Hague, The Netherlands, Oct., 1995, 271–279.
44. M. Hughes, R.T. Barton, S.A.G.R. Karunathikala, N.A. Hampson, R. Leek, The residual capacity estimation of fully sealed 25 Ah lead/acid cells, *J. Power Sources*, **17**, 305–329, 1986.
45. Y. Konya, T. Takeda, K. Takano, M. Kohno, K. Yutsimoto, T. Ogata, A deterioration estimating system for 200-Ah sealed lead-acid batteries, *Proc. Int. Telecomm. Energy Conf.*, Vancouver, Canada, Oct., 1994, 256–262.
46. J. Alzieu, J. Leroy, A. Vicaud, Un parametre de controle de l'état d'une batterie d'accumulateurs en service: la resistance électrique interne, *Société des Electriciens et Electroniciens, Journées Gaston Planté*, Gif-sur-Yvette, France, Nov. 1989, 213–217.
47. D. Wilson, The measurement of ripple current in battery plants, *Proc. Int. Telecomm. Energy Conf.*, San Diego, Oct. 30-Nov. 2, 1988, 374–378.
48. D. Berndt, Electrochemical energy storage: principles, state of the art and future possibilities, *Varta Special Report*, 4, 1987.
49. R.S. Robinson, System noise as a signal source for impedance measurements on battery strings, *Proc. Int. Telecomm. Energy Conf.*, Paris, Sept. 1993, 365–368.
50. F.A. Laws, *Electrical Measurements*, McGraw Hill Book Comp., 2nd ed., New York: McGraw-Hill, 1938, p. 328.
51. I. Damlund, Analysis and interpretation of AC-measurements on batteries used to assess state-of-health and capacity condition, *Proc. Int. Telecomm. Energy Conf.*,The Hague, The Netherlands, Oct., 1995, 828–833.
52. J.B. Copetti, F. Chenlo, Internal resistance characterization of lead-acid batteries for PV rates, *11th Photovoltaic Solar Energy Conf.*, Montreux, Switzerland, Oct. 1992, 1116–1119.
53. Gl. Albér, Impedance testing ¯ is it a substitute for capacity tests?, *Proc. Int. Telecomm. Energy Conf.*, Vancouver, Canada, Oct. 1994, 245–249.
54. V.A. Tyagai, Faradaic noise of complex chemical reactions, *Electrochimica Acta*, **16**, 1971, 1647–1654.
55. E.M. Lehockey, A.M. Brennenstuhl, G. Palumbo, P. Lin, Electrochemical noise for evaluating susceptibility of lead-acid battery electrodes to intergranular corrosion., *British Corrosion J.*, **33**, 1988, 1, 29–36.
56. S. Martinet, R. Durand, P. Ozil, P. Leblanc, P. Blanchard, Application of electrochemical noise analysis to the study of batteries: state-of-charge determination and overcharge detection, *J. of Power Sources*, **83**, 1999, 93–99.
57. D.H.J. Baert, A.A.K. Vervaet, Determination of the state-of-health of VRLA batteries by means of noise measurements, *Proc. Int. Telecomm. Energy Conf*, Edinburgh, U.K., Oct. 2001, 301–306.
58. I. Buchmann, *Batteries in a portable world*, Cadex Electronics Inc. cadex
59. K.S. Champlin, K. Bertness, A fundamentally new approach to battery performance analysis using DFRA/DFIS technology, *Proc. Int. Telecomm. Energy Conf.*, Phoenix, AZ, Sept., 2000, 348–355.
60. D.H.J. Baert, A.A.K. Vervaet, A new method for the measurement of the double layer capacitance for the estimation of battery capacity, *Proc. Int. Telecomm. Energy Conf.*, Edingburgh, U.K., Oct 2003, 733–738.

Cross-references

See Secondary cells

See Uninterruptable power supplies

Related Encyclopedia titles.

Secondary cells; Telecommunication power supplies; Uninterruptable power supplies; Solar power stations; ***Battery storage plants***; ***Electrochemical electrodes***; ***Electric impedance***; ***Electric current measurements***; ***Voltage measurements***; ***Automatic test equipment***

DANIËL H. J. BAERT
Department of Electronics and Information Systems Gent University,
Sint-Pietersnieuwstraat, 41
B-9000, Ghent, Belgium